Co and Al co-doping for ferromagnetism in ZnO:Co diluted magnetic semiconductors

2009 J. Phys.: Condens. Matter 21 056002

(http://iopscience.iop.org/0953-8984/21/5/056002)

J. Phys.: Condens. Matter **21** (2009) 056002 (5pp) doi:10.1088/0953-8984/21/5/056002

Co and Al co-doping for ferromagnetism in ZnO:Co diluted magnetic semiconductors

G S Chang[1], E Z Kurmaev[2], D W Boukhvalov[2,3], L D Finkelstein[2], A Moewes[1], H Bieber[4], S Colis[4] and A Dinia[4]

[1] Department of Physics and Engineering Physics, University of Saskatchewan, 116 Science Place, Saskatoon, SK, S7N 5E2, Canada
[2] Institute of Metal Physics, Russian Academy of Sciences-Ural Division, 620041 Yekaterinburg, Russia
[3] Institute for Molecules and Materials, Radboud University, nl-6525 ED Nijmegen, The Netherlands
[4] IPCMS CNRS-UMR 7504 (ULP-ECPM), 23 rue du Loess, F-67034, Strasbourg Cedex, France

E-mail: gapsoo.chang@usask.ca

Received 14 August 2008, in final form 25 November 2008
Published 12 January 2009
Online at stacks.iop.org/JPhysCM/21/056002

Abstract
Co and Al co-doped ZnO diluted magnetic semiconductors are fabricated by a pulsed laser deposition and their electronic structure is investigated using x-ray absorption and emission spectroscopy. The $Zn_{0.895}Co_{0.100}Al_{0.005}O$ thin films grown under oxygen-rich conditions exhibit ferromagnetic behavior without any indication of Co clustering. The Co L-edge and O K-edge x-ray absorption and emission spectra suggest that most of the Co dopants occupy the substitutional sites and the oxygen vacancies are not responsible for free charge carriers. The spectroscopic results and first principles calculations reveal that the ferromagnetism in Co and Al co-doped ZnO semiconductors mainly arises from Al interstitial defects and their hybridization with Co substitutional dopants.

1. Introduction

Diluted magnetic semiconductors (DMSs) based on ZnO have recently been attracting much attention, because transition metal (TM) doped ZnO DMSs exhibit ferromagnetism at room temperature (RT) in contrast to those based on III–V semiconductors such as GaAs and InAs [1, 2]. Another advantage of using ZnO as a host semiconductor is related to its wide band-gap in the ultraviolet region (about 3.36 eV), which opens the possibility for the development of spin-optoelectronic devices. However, the experimental results for the magnetic properties of ZnO-based DMS systems are quite controversial, and the origin of ferromagnetism is yet to be elucidated (see [3–10]). One key question in understanding the ferromagnetic behavior of ZnO-based DMS materials is the identification of defects which lead to free carriers, since the ferromagnetism of DMSs is supposed to depend on the existence of delocalized carriers that can hybridize with the localized spins of magnetic impurity atoms and provide exchange coupling between d-spins localized on magnetic atoms [11, 12].

Free electrons can be introduced into TM-doped oxide semiconductors by growing the samples under oxygen-deficient conditions (controlled by the partial oxygen pressure during sample preparation) or by co-doping with an element from the third group (e.g. B, Al, Ga or In). On the other hand, it has recently been shown that the ZnO:Co DMS promises to have a high Curie temperature (T_C) due to free charge carriers induced by TM interstitials rather than oxygen vacancies [2]. This is in accordance with first principles electronic structure calculations suggesting that both electron-doping with Zn interstitials and hole-doping with oxygen vacancies can make ZnO:Co and ZnO:Mn DMSs magnetically robust [13].

In the present paper we have used Co and Al co-doping to induce a strong ferromagnetism in ZnO. The electronic structure of ZnO thin films co-doped with Co and Al was investigated using synchrotron-excited x-ray absorption and emission spectroscopy (XAS and XES, respectively). The O 1s

Table 1. Synthesis parameters and physical properties of $Zn_{0.895}Co_{0.100}Al_{0.005}O$ thin films.

Sample	Pressure (Torr)	Oxygen flow rate (sccm)	M_S (μ_B/Co atom) 5 K	M_S (μ_B/Co atom) 300 K	$I(L_2)/I(L_3)$
1	6.0×10^{-7}	0	1.45	0.58	1.14
2	3.6×10^{-5}	0.35	0.79	0.08	1.33
3	5.6×10^{-4}	5	1.00	0.30	1.34

XAS and O Kα XES spectra show that the number of oxygen vacancies in the Co and Al co-doped ZnO thin films does not change under variation of the partial oxygen pressure during sample preparation, while the magnetic properties of samples are significantly influenced by the partial oxygen pressure. It is shown that nonresonant and resonant Co $L_{2,3}$ XES can be used as a tool to estimate the local environment around magnetic dopant ions in oxide-based DMS materials.

2. Experimental details

The $Zn_{0.895}Co_{0.100}Al_{0.005}O$ target was synthesized by a co-precipitation technique and sintered at 800 °C for 15 min. Then, Co and Al co-doped ZnO thin films with a thickness of about 150 nm were deposited on $A1_2O_3(0001)$ substrates by pulsed laser deposition (PLD) using a KrF excimer laser. During the PLD process, a background oxygen gas pressure was used in order to evaluate the effect of partial oxygen pressure on the physical properties of $Zn_{0.895}Co_{0.100}Al_{0.005}O$ thin films. For (oxygen-deficient) sample 1, the pressure was kept at 6.0×10^{-7} Torr without oxygen flow. The (oxygen-rich) samples 2 and 3 were prepared in a partial oxygen pressure of 3.6×10^{-5} Torr (with an oxygen flow rate of 0.35 sccm) and 5.6×10^{-4} Torr (5 sccm), respectively. For all samples, the laser frequency and energy density were kept constant at 10 Hz and 1 J cm^{-2}, respectively. The target–substrate distance was 5 cm. The growth temperature was set at 500 °C in order to improve the crystalline quality of $Zn_{0.895}Co_{0.100}Al_{0.005}O$ thin films. The preparation parameters are presented in table 1.

X-ray diffraction (XRD) measurements were performed using a Siemens D500 diffractometer working in the θ–2θ configuration and equipped with a Co source (Kα_1 = 0.178 89 nm). The magnetic properties were investigated using a superconducting quantum interference device (SQUID). Zero-field-cooled (ZFC) and field-cooled (FC) magnetization (M–T) curves from 2 to 300 K were measured with an applied field of 1 kOe and the magnetic hysteresis (M–H) loops were recorded at 5 and 300 K. The magnetic field was applied parallel to the sample surface. The diamagnetic contribution of the $A1_2O_3$ substrate was corrected in the presented magnetization loops.

The XAS and XES measurements were carried out at Beamline 8.0.1 of the Advanced Light Source at the Lawrence Berkeley National Laboratory, Berkeley, CA, USA. Resonant Co $L_{2,3}$ (3d4s $\rightarrow$ 2p transition) XES spectra were obtained at an excitation energy (E_{exc}) near the L_2 absorption thresholds. On the other hand, nonresonant Co $L_{2,3}$ and O Kα (2p $\rightarrow$ 1s transition) XES spectra were measured at E_{exc} well above the absorption thresholds. All spectra were recorded at RT and normalized to the number of photons falling on the sample monitored by a highly transparent gold mesh.

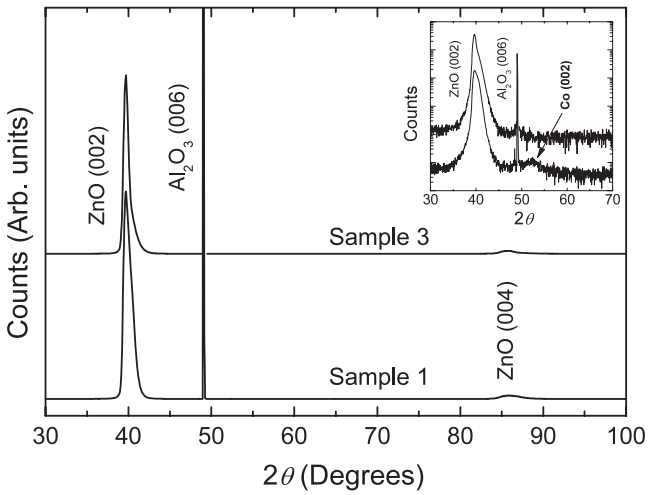

Figure 1. XRD patterns of $Zn_{0.895}Co_{0.100}Al_{0.005}O$ thin films prepared under oxygen-deficient (sample 1) and oxygen-rich (sample 3) conditions. The inset shows the same data replotted on a semilogarithmic scale.

3. Results and discussion

Figure 1 shows the XRD patterns of $Zn_{0.895}Co_{0.100}Al_{0.005}O$ thin films deposited on $Al_2O_3(0001)$ substrates. Two multiple-diffraction peaks suggest that all films are epitaxially grown along the [001] direction (out of plane) with a wurtzite structure. The Al_2O_3 substrate peak has been cut for more clarity. One can see that sample 1 prepared under oxygen-deficient conditions shows a peak at 52.5° corresponding to the (0002) plane of the Co hcp phase (see the inset in figure 1). This peak is not found in the other samples grown under an oxygen atmosphere. The presence of metallic Co clusters in sample 1 only is also confirmed by the ZFC/FC measurements. The M–T magnetization curve in the inset of figure 2(a) shows a ferromagnetic to superparamagnetic transition with a blocking temperature of 10 K for sample 1, whereas other samples present superposed ZFC and FC curves in the inset of figure 2(b). Furthermore, the M–H hysteresis loop of sample 1 has higher coercive field and remanent magnetization at 5 K (figure 2(a)) than those of oxygen-rich samples (samples 2 and 3). The saturated magnetization (M_S) was recorded at an applied field of 50 kOe. M_S of sample 1 is found to be 1.45 μ_B/Co atom at 5 K and decreases to 0.58 μ_B/Co atom at 300 K. We should note that even the samples showing no

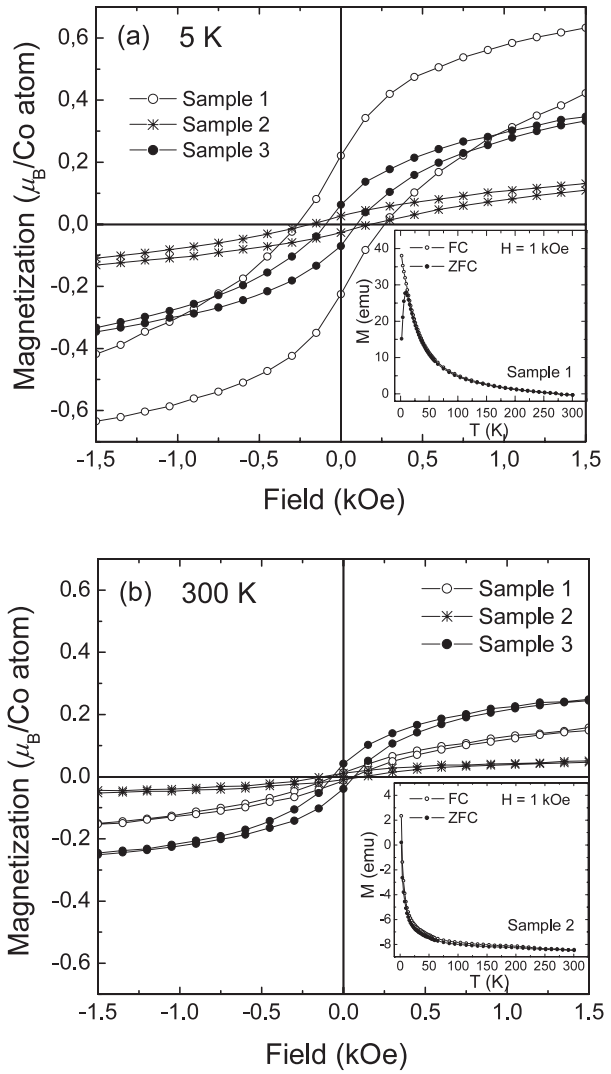

Figure 2. M–H curves of $Zn_{0.895}Co_{0.100}Al_{0.005}O$ thin films at 300 and 5 K. The insets in (a) and (b) show the ZFC/FC curves of samples 1 and 2, respectively.

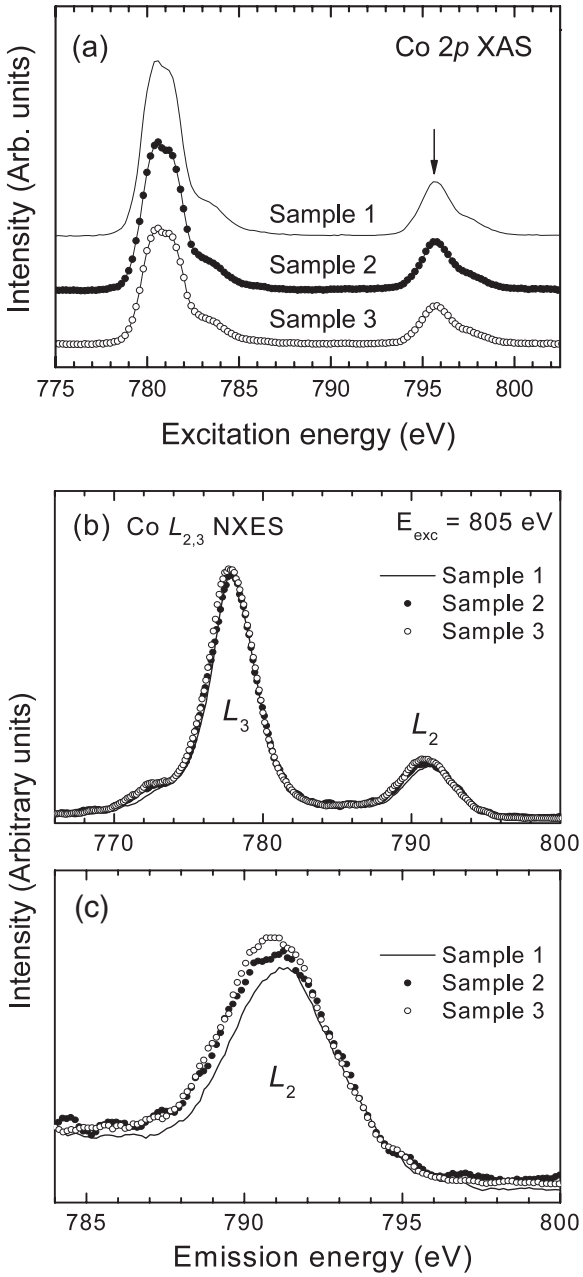

Figure 3. Co 2p XAS spectra (a) and Co $L_{2,3}$ nonresonant x-ray emission spectra (b) of $Zn_{0.895}Co_{0.100}Al_{0.005}O$ thin films. The detailed spectra in the vicinity of L_2 emission line are presented in (c).

indication of metallic Co clusters (samples 2 and 3) exhibit ferromagnetic behavior at both 5 and 300 K. The M_S values of samples 2 and 3 are 0.79 and 1.00 μ_B/Co atom (at 5 K) and 0.08 and 0.30 μ_B/Co atom (at 300 K), respectively (see table 1). This is direct evidence that ferromagnetic behavior of oxygen-rich samples 2 and 3 is not caused by Co aggregation.

Figure 3 presents Co 2p XAS spectra (measured in TEY mode) and Co $L_{2,3}$ nonresonant x-ray emission spectra (NXES) of $Zn_{0.895}Co_{0.100}Al_{0.005}O$ thin films prepared at different partial oxygen pressures. The NXES spectra were recorded at E_{exc} of 805 eV, well above the Co 2p absorption threshold. Although the Co 2p XAS spectra are almost identical for all samples, there is a noticeable change in the Co $L_{2,3}$ NXES spectra. The relative intensity ratio of L_2 to L_3 emission lines $[I(L_2)/I(L_3)]$ systematically decreases with decreasing partial oxygen pressure (see figure 3(c)). All spectra have been normalized to the L_3 emission line. In principle, the decrease in $I(L_2)/I(L_3)$ intensity ratio is related to a reduction in the L_2-holes in $3d \rightarrow 2p_{1/2}$ transitions and an increase in L_3-holes in $3d \rightarrow 2p_{3/2}$ transitions during the x-ray emission process. According to our previous studies [10–12], the $I(L_2)/I(L_3)$ intensity ratio is strongly affected by the number of free carriers around the target element (Co in our case), and the reduction of L_2 states in metallic Co arises from radiationless $L_2L_3M_{4,5}$ Coster–Kronig (CK) transitions. In the CK process, a L_2 hole passes on the less excited L_3 level and the resulting energy is transferred to either the $3d(M_{4,5})$ electron for the individual Auger transition within the same atom or the collective electron density (not necessarily d-symmetry) for the excitation of plasma oscillations. The latter CK mechanism is in addition to the main one and its probability is increased with the number of free carriers. Therefore, the $I(L_2)/I(L_3)$

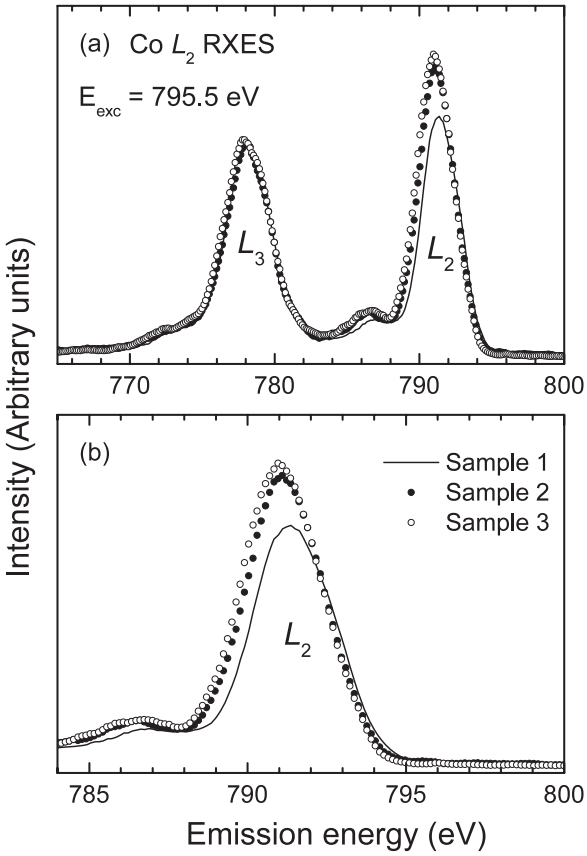

Figure 4. (a) Co $L_{2,3}$ XES spectra of $Zn_{0.895}Co_{0.100}Al_{0.005}O$ samples resonantly excited at L_2 absorption. The detailed spectra in the vicinity of L_2 emission line are presented in (b).

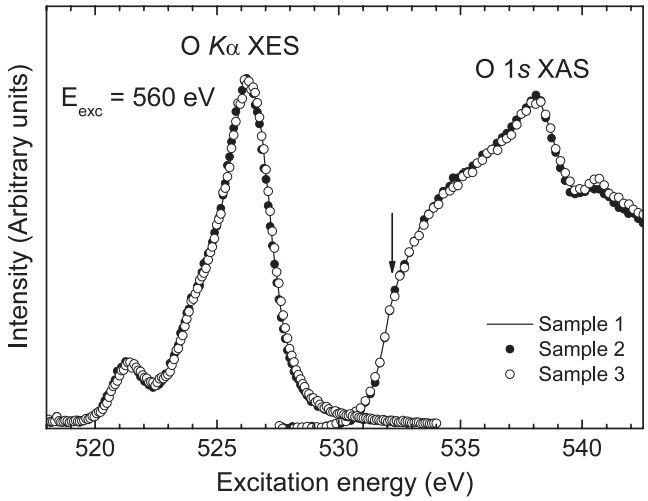

Figure 5. O 1s XAS and nonresonant O Kα XES spectra of $Zn_{0.895}Co_{0.100}Al_{0.005}O$ thin films.

intensity ratio provides an efficient way of characterizing the variation in charge carriers and metallicity of 3d-based DMS systems.

In addition, since the $I(L_2)/I(L_3)$ intensity ratio is inversely proportional to the ratio of total photoabsorption coefficients for excitation energies at the L_2 and L_3 threshold [14], the suppression of the $I(L_2)/I(L_3)$ intensity ratio due to the CK process becomes more prominent in the L_2 resonant regime than nonresonant XES. This was previously confirmed by a fact that for the L_2 resonant excitation, the $I(L_2)/I(L_3)$ intensity ratio of metallic Co (0.62) is much smaller than for insulating CoO (1.45) [15, 16]. A similar tendency can be seen in resonant Co $L_{2,3}$ XES spectra (RXES) excited at the L_2 threshold (E_{exc} = 795.5 eV), as shown in figure 4. Sample 1 has the lowest $I(L_2)/I(L_3)$ intensity ratio, which is much smaller than that in the NXES spectrum. This agrees well with the XRD results suggesting that a some of the Co dopants form metallic clusters. On the other hand, the lower $I(L_2)/I(L_3)$ intensity ratios of samples 2 and 3 (1.33 and 1.34, respectively) than that of CoO (1.45) suggest that a significant number of free d carriers are still present in the Co and Al co-doped ZnO samples.

Although the XRD and XES results reveal the presence of Co clusters in sample 1 causing the ferromagnetic behavior, ferromagnetism in samples 2 and 3 still needs to be explained in terms of the contribution from free charge carriers. As already mentioned, free charge carriers can be introduced into ZnO:Co by oxygen vacancies and/or Al co-dopants. Figure 5 shows the O 1s XAS and O Kα XES spectra of $Zn_{0.895}Co_{0.100}Al_{0.005}O$ samples. One can see that change in the oxygen atmosphere is not accompanied by any difference in either XAS or XES spectra. According to Song *et al* [17], the presence of an oxygen vacancy in ZnO:Co enhances the spectral intensity near the absorption edge (around 523 eV) in the O 1s XAS spectrum (see the arrow in figure 5). We have not found such change in our samples, and therefore we can exclude that free carriers in samples 2 and 3 are connected with oxygen vacancies.

Based on the spectroscopic results, we estimate that the presence of free charge carriers is related to the doping of Al into ZnO:Co. That is why we have also performed calculations of the formation energies (E_{Form}) for several Al-related defects and their magnetic properties in the same way as was done for the polycrystalline $Zn_{1-x}Co_xO$ system [18]. The linearized muffin-tin-orbital method in the atomic sphere approximation (LMTO-ASA) within the local spin-density approach (LSDA) was used by employing a supercell geometry with 64 atoms in the cell ($4a \times 4a \times 4c$). The defect configurations considered and the calculation results are presented in table 2. The E_{Form} of Zn interstitials [Zn(I)] was also calculated and compared to those of our model configurations, because the Zn(I) defects are also known to induce free electrons in ZnO:Co. The calculated formation energy of Zn(I) is 2.12 eV, which is much higher than those of Al-related defects (0.78–2.05 eV). Therefore, the occupation of Zn(I) defects is energetically unfavorable. One interesting thing is that the presence of oxygen vacancies significantly increases the formation energy of all types of defect. This means that in the Co and Al co-doped ZnO DMSs, the oxygen vacancies are relatively difficult to be formed. It is in accordance with the XAS results of O 1s spectra as shown in figure 5. On the other hand, a high value of the ferromagnetic exchange interaction is obtained in the nCo(S)–Al(I) configuration (where n = 2 or 3) with T_C of 306–320 K. The formation energies for these

Table 2. Calculated formation energies and magnetic properties for different defect configurations.

Defect	Formation energy (eV per atom)		Exchange interaction (meV)	Curie temperature (K)
	Without O_V [a]	With O_V		
2Co(S)–Al(I)	2.05	2.06	+24	306
3Co(S)–Al(I)	0.935	1.64	+13	320
Co(S)–Al(S)–Co(S)	0.78	2.06	−6	75

[a] O_V represents an oxygen vacancy.

configurations are 2.05 (for $n = 2$) and 0.935 ($n = 3$) eV per atom. Although the Co(S)–Al(S)–Co(S) configuration has an even lower formation energy of 0.78 eV per atom, it exhibits only antiferromagnetic exchange interaction. From the overall results, we suggest that a strong ferromagnetism in the Co and Al co-doped ZnO thin films is mainly related to the presence of Al interstitial atoms and these Al defects enhance the exchange interaction between Co neighbors by forming small clusters. Such clusters, containing only several atoms, cannot be detected by a XRD technique due to its low sensitivity [19]. Therefore, the XAS and XES studies can complement the deficiency of XRD analysis and give insight into the local environment around magnetic atoms in various DMS materials because they are sensitive to the first coordination sphere of target element.

4. Conclusion

In conclusion, we have investigated the magnetic properties and electronic structure of Co and Al co-doped ZnO DMSs. The Co L-edge and O K-edge XAS and XES spectra of $Zn_{0.895}Co_{0.100}Al_{0.005}O$ thin films reveal that some Co dopants are involved in the Co clustering when a sample is prepared in an oxygen-deficient regime. However, ferromagnetic behaviors are observed in the oxygen-rich samples without any indication of Co aggregation by XRD. According to the first principles calculations, free carriers are present due to Al interstitials rather than oxygen vacancies and the Al interstitial-related defect configuration can cause a strong ferromagnetic exchange interaction. The overall results suggest that ferromagnetism in Co and Al co-doped ZnO is strongly related with the interstitial occupancy of Al dopants which involve the formation of micro-clusters containing only several Co and Al atoms.

Acknowledgments

We gratefully acknowledge the Russian Academy of Sciences Program (project 01.2.006 13395), the Natural Sciences and Engineering Research Council of Canada (NSERC) and the Canada Research Chair program. This work is also partly supported by the Russian Science Foundation for Basic Research (projects 08-02-00148 and 06-02-16733) and the Research Council of the President of the Russian Federation (grants NSH-1929.2008.2 and NSH-1941.2008.2). HB would like to thank the Region Alsace for financial support. DWB acknowledges a support from Stichting voor Fundamenteel Onderzoek der Materie (FOM), the Netherlands.

References

[1] Ueda K, Tabata H and Kawai T 2001 *Appl. Phys. Lett.* **79** 988
[2] Dinia A, Schmerber G, Mény C, Pierron-Bohnes V and Beaurepaire E 2005 *J. Appl. Phys.* **97** 123908
[3] Coey J M D, Venkatesan M and Fitzgerald C B 2005 *Nature* **4** 173
[4] Sharma P, Gupta A, Rao K V, Owens F J, Sharma R, Ahuja R, Osorio Guillen J M, Johansson B and Gehring G A 2003 *Nat. Mater.* **2** 673
[5] Rao C N and Deepak F L 2005 *J. Mater. Chem.* **15** 573
[6] Kittilstved K R, Liu W K and Gamelin D R 2006 *Nat. Mater.* **5** 291
[7] Cheng X M and Chien C L 2003 *J. Appl. Phys.* **93** 7876
[8] Bouloudenine M, Viart N, Colis S and Dinia A 2004 *Chem. Phys. Lett.* **397** 73
[9] Alaria J, Bouloudenine M, Schmerber G, Colis S, Dinia A, Turek P and Bernard M 2006 *J. Appl. Phys.* **99** 08M118
[10] Belghazi Y, Schmerber G, Colis S, Rehspringer J L, Berrada A and Dinia A 2006 *Appl. Phys. Lett.* **89** 122504
[11] Pearton S J, Norton D P, Ip K, Heo Y W and Steiner T 2005 *Prog. Mater. Sci.* **50** 293
[12] Chambers S A 2006 *Surf. Sci. Rep.* **61** 345
[13] Sluiter M H F, Kawazoe Y, Sharma P, Inoue A, Raju A R, Rout C and Waghmare U V 2005 *Phys. Rev. Lett.* **94** 187204
[14] Kurmaev E Z, Ankudinov A L, Rehr J J, Finkelstein L D, Karimov P F and Moewes A 2005 *J. Electron Spectrosc. Relat. Phenom.* **148** 1
[15] Chang G S, Kurmaev E Z, Boukhvalov D W, Finkelstein L D, Kim D H, Noh T-W, Moewes A and Callcott T A 2006 *J. Phys.: Condens. Matter* **18** 4243
[16] Grebennikov V I 2002 *Surf. Invest. X-ray Synchrotron Neutron Tech.* **11** 41
[17] Song C, Pan S N, Liu X J, Li X W, Zeng F, Yan W S, He B and Pan F 2007 *J. Phys.: Condens. Matter* **19** 176229
[18] Chang G S, Kurmaev E Z, Boukhvalov D W, Finkelstein L D, Colis S, Pedersen T M, Moewes A and Dinia A 2007 *Phys. Rev.* B **75** 195215
[19] Kobayashi M, Kuma R and Morita A 2006 *Catal. Lett.* **112** 37